Surface and Coatings Technology, Volume 204, Issues 16-17, 15 May 2010, Pages 2624-2631

Accepted Manuscript

Investigation of the Thermal Field in Micro Friction Surfacing

V.I. Vitanov, N. Javaid

PII: S0257-8972(10)00083-6
DOI: doi: 10.1016/j.surfcoat.2010.02.003
Reference: SCT 15520

To appear in: *Surface & Coatings Technology*

Received date: 13 July 2009
Accepted date: 2 February 2010

Please cite this article as: V.I. Vitanov, N. Javaid, Investigation of the Thermal Field in Micro Friction Surfacing, *Surface & Coatings Technology* (2010), doi: 10.1016/j.surfcoat.2010.02.003

Investigation of the Thermal Field in Micro Friction Surfacing

V.I. Vitanov[1], N. Javaid[2]

1

School of Engineering, Durham University, Durham DH1 3LE (corresponding author)

2

School of Applied Sciences, Cranfield University, Cranfield, MK43 0AL, United Kingdom

E-mail v.i.vitanov@durham.ac.uk Office tel. ++44 1913342377 Fax: ++44 1913342390

Abstract

To model the thermal response of the micro friction surfacing process with complex geometries and to tackle transient deposition processes, suitable numerical methods have been developed. The approach of coupled transient thermal analysis to account for the temperature fields generated during the dwell and deposition phases of the process resulted in reasonably accurate results, with an error of 18% between absolute maximums. The major discrepancy between the experimental and simulated results occurred at locations with a change in substrate geometry. The heat distribution profile at the frictional interface and variation in material properties with temperature could have significant effects on the thermal response.

Keywords: Coating, Thermal modeling, Friction surfacing.

1. Introduction

Friction surfacing is an important surface engineering technique used for obtaining various hard metal coatings for numerous practical applications. It involves rotating a rod of the coating material onto a substrate under the action of external load the frictional heat generated at the rubbing interface is sufficient to deposit a layer of hot plasticized metal on a substrate. Common to many other processes, friction surfacing involves a moving heat source and the temperature field created at the bond interface, influences the diffusion rates at the deposit-substrate interface, which subsequently will determine the strength of the bond [1, 2]. Several closed form mathematical models of moving circular or elliptical heat sources have been reported [3 through 9,14], however the limitations of these models with changing boundary conditions, temperature dependence of physical parameters and complex geometry makes them less practical for present application. In the present study a numerical model and its validation against the experimental results is presented.

Insert Nomenclature

1.1 Process parameters

The figure 1 shows the process parameters categorized into three main categories that are process inputs, state indicators and process outputs [11, 12, 13]. Another important factor that will significantly affect the process is the temperature field generated in the substrate which in turn will define the bond interface temperature.

Insert figure1

The rotational speed (*rpm*) and feed rate of mechtrode (V_z) and the traverse rate of the substrate (V_x) are the essential machine input parameters. A particular combination of these input parameters will be most suitable for a particular application. Force (F_n) and substrate temperatures (T_1, T_2, T_3, T_4) at specific locations are the measurable in process parameters which are indicative of the state of the process. Bond strength (S), coating thickness (T) and width (W) are the necessary process outputs that cannot be measured or quantified during the process. The bond interface temperature as a result of temperature field generated in the

substrate is responsible for successful deposition. Since this temperature cannot be measured directly by contact or non contact methods, an indirect approach is to resort to thermal modeling to identify it.

2. Process phases and analytical models for generated frictional heat

One of the basic problems while modeling such a process with numerical methods lies with the identification of generated heat at frictional interface that can be used as a boundary condition for determining bulk temperature fields. The approach normally employed involves the development of a mathematical relation for instantaneous frictional heat generation over an infinitesimal area based on the process dynamics. The total frictional heat is evaluated by integrating the developed relation over whole of the frictional interface. The heat generated during friction surfacing process is a certain fraction of the total mechanical energy input, which can be quantified by the amount of work per unit time (power) expended in overcoming developed frictional force at the interface, under the prevailing process conditions.

The process is characterized by two distinct phases and since process dynamics changes from one phase to another, mathematical models for each phase have been developed. These relations are based on the assumptions of constant pressure and exponential decay [7, 10, 13] of coefficient of friction with sliding velocity.

$$M_{dwell} = \frac{4\mu_o \eta F_n}{c^3 \omega^3 R^2} e^{-c\omega R} \quad (1)$$

$$P_{dwell} = \frac{4\mu_o \eta F_n}{c^3 \omega^2 R^2} e^{-c\omega R} \quad (2)$$

$$M_{depo} = \frac{16\mu_o \eta F_n}{\sqrt{2}\pi c^3 \omega^3 R^2} e^{-c\omega R} \quad (3)$$

$$P_{depo} = \frac{16\mu_o \eta F_n}{\sqrt{2}\pi c^3 \omega^2 R^2} e^{-c\omega R} \quad (4)$$

Where

$$\eta = \left(e^{c\omega R} - \frac{c^2\omega^2 R^2}{2} - Rc\omega - 1 \right)$$

The above developed expressions (1 through 4) were used to predict frictional heat generated during the process. The detail of symbols and abbreviations used are listed in nomenclature (section 1).

3. Experimental Measurements

A dedicated setup was developed for measuring force and temperatures during experimentation. Thermocouples were used for temperature measurements and were placed at specific locations at the bottom surface of substrate, coincident with the deposit centerline along the traverse direction. The setup was designed to be repetitive; therefore, the deposition always started 5mm before the first thermocouple during every experimental run. The figure2 shows the exact locations of the thermocouples, this placement ensured that the temperature profile was recorded at two points on each part of the substrate (thicker part and thinner part) over the entire deposit length.

Insert figure 2

The temperature and force records produced from the acquisition system for each experimental run were saved as Excel's spread sheets for analysis and for validation of thermal model. The temperature and force plots are shown below, which were used for FEM thermal study.

Insert figure 3

Three different force values related to points B, C and D for the deposition phase of the process can be identified from the above plot. Logically an average over these values should suffice but the difference in force at points B and C (1660 N) is such that an average force in excess of 500N will be defined over the relatively steady force between points C and D. Considering the force application durations, force at B gradually reduces to force at C within 4.75 seconds after the start of phase II, afterwards, it remains reasonably steady from point C

to D for 20.25 seconds of the process. Therefore, an average value of force evaluated over the steady portion of force-time curve will be used for the calculation of generated frictional heat.

Insert figure 4

4.0 FEM thermal modeling

The finite element method is based on integral minimization of error, which is quite different from the finite difference method based on Taylor series expansion. The main advantage of using the finite element method is that it allows for unstructured meshes and hence, highly irregular geometries can be handled. Further, values of the unknown can be generated continuously across the entire solution domain rather than at isolated points. TMG Thermal Analysis (Ideas Simulation Software) was used for modeling purposes. It has the capability of simulating heat transfer by conduction, convection, radiation, fluid flow, and phase change.

4.1 Prerequisites

The dwell phase is characterized by a stationary mechtrode (not traversing) and the heat flux is applied over a specific region of the substrate. The period or duration of this phase varies with materials used for coating and substrate, normally it is between 4 to 8 seconds. Considering the short duration of this preheat stage transient mode of analysis was adopted with simulation time equivalent to the preheat time. During the deposition phase the mechtrode movement over the substrate makes it a moving heat source problem involving heat and mass transfer, hence the transient mode of analysis was considered. The system defined for the thermal study constituted following essential components and interactions.

- Coating material rod
- Deposit
- Substrate
- Clamping device
- Interaction between coating material rod and machine spindle chuck

- Interaction between substrate bottom surface and holding device mounted on the machine bed.
- Interaction at the rubbing interface between the rotating rod and the deposit
- Interaction between the deposit and the substrate
- Interaction between the system and the surrounding fluid (air)

The mentioned components of the system defined the geometric entities of the model and the interactions described the boundary conditions to be applied to the geometric model for thermal analysis. For realistic comparison between the simulation and experimental results, the modeled geometry has to be close to the real geometry of the components with minimum simplifications. However, certain details that are considered less significant are always omitted to simplify the model. The geometric simplifications that were made during the modeling process are listed below:

- The area due to the cold laps was ignored, and the width of the deposit was taken equal to the effective heat generation area of the mechtrode.
- The flash over the cylindrical surface of the mechtrode was ignored.
- The thickness of the deposit was assumed to be uniform.

The figure below is the diagrammatic representation of the factors that were considered before modeling the process.

Insert figure 5

4**.2 Geometric modeling**: The shape and the true dimensions of the substrate as shown in figure 2 were modeled. The deposit of uniform thickness, width equal to the approximate effective diameter of the rubbing interface and length equal to that obtained during actual run were modeled. The coating layer was discretised into crescent shaped volumes and the successive addition of these volumes indicated the coating deposition (figure 6).

Insert figure 6

The location of modeled deposit has the same physical orientation on the substrate as obtained

during experimental runs. Figure 7 shows the composite model prepared by adding the deposit layer onto the top surface of the substrate.

Insert figure 7

For a deposit length of 30mm, thirty crescent shaped volumes were created each bounded by two horizontal crescent shaped and two vertical semi circular surfaces. The mechtrode was modeled by a simple cylindrical shape without considering the flash around the peripheral region. To simulate the dynamic changes in length during each step of the process, the mechtrode cylindrical volume was sectioned to create individual discs with thickness equal to the change in mechtrode length based on the computed time interval ($\Delta z = \Delta x(V_z/V_x)$). The figure 8 shows the modeled geometry;

Insert figure 8

For a mechtrode of 25mm in length, 125 circular disc shaped volumes were created with every individual volume bounded by two horizontal circular surfaces and one vertical cylindrical surface. The clamping device (heat sink) has no physical significance apart from acting as a heat sink in a thermal model, therefore, the geometric representation involved only a rectangular surface in contact with the bottom surface of substrate. The figure 9 shows the complete geometric model used for thermal analysis.

Insert figure 9

4.3 Material Properties

The process essentially involves two types of materials, a coating material and the material of the substrate, although these materials can be identical but in most of the applications they are different depending on the required surface properties. The material properties of the substrate (subs) and coating (coat) are listed below:

Insert Table 1: Material properties of Stellite 6 and SS 316

The values for these properties have been obtained from literature based on average

temperature and on the assumption that the materials are isotropic (uniform properties in all directions).

4.4 Meshing

All the surfaces of individual components were meshed first with linear triangular shell elements and then the volumes of corresponding components were meshed associatively, with linear tetrahedral elements, so that the nodes of the solid elements are shared by the thin shell elements (surface coats) at the surface. An important aspect that needed attention in particular was the location of thermocouples on the substrate surface as available from the experimental setup. This location had to be represented accurately on the geometric model so that the elemental nodes could be placed at those specific points facilitating the extraction of simulation data for comparison and validation against experimental data (based on the same geometric location).

Insert figure 10

Free meshing creates nodes and elements based on the element type, element length and the meshing algorithm selected, though the meshing densities at specific locations can be controlled based on the geometric model but the placement of nodes at exact locations is rather difficult. Therefore, anchor nodes were created which forced the free meshing operation to place elemental nodes at those specific points. The figure 10 shows the location of thermocouples where the anchor nodes were created and the generated FEM model.

4.5 Boundary Conditions

The boundary conditions were applied directly to geometric groups created during modeling of the system, referencing the associated finite element entities. The following boundary conditions were applied to the geometric entities

- Interface between the mechtrode and machine spindle chuck-Constant Temperature

- Substrate holding device attached to the machine table-Constant Temperature
- Mechtrode frontal surface in contact with the deposit-Heat load boundary condition.
- Free convection from the substrate surfaces
- Free convection from the deposit surfaces
- Forced convection from the mechtrode cylindrical surface

Following types of thermal couplings were used based on the interface:

4.5.1 Resistance Coupling.

- Between the bottom surface of substrate and clamping device.

4.5.2 Constant Coefficient Coupling.

- Between mechtrode contact surface and the deposit top surface.
- Between mechtrode (where flash is formed) and the non geometric air element to simulate an enhanced heat transfer affect due to the flash formation.

4.5.3 Conductive Interface Coupling.

- Between bottom surface of deposit and the portion of the top surface of substrate associated with it.

4.6 Functional Relationship

The simulated deposit layer ahead of the mechtrode does not exist prior to the deposition process. Therefore, to model this effect the coating layer was discretised into crescent shaped volumes and “birth and death” method was used to deactivate and activate elements throughout the analysis. In our study this was achieved by varying thermal conductivity of the elements associated with each volume at predefined intervals ($\Delta t = \Delta x/V_x$) validated against the experimental results. The thermal conductivity of elements ahead of mechtrode is considered negligible and just at the instant before the mechtrode is about to move over the element the conductivity switches to its specified value thus representing the physical

behavior of the friction surfacing process.

Insert figure 11

The above plot shows the linear increase in thermal conductivity of a group of finite elements within a crescent shaped volume during the calculated time step. The number of functions defined was equivalent to the number of volumes into which the deposit was divided.

4.7 Run Time Parameters

To simulate the traverse of the substrate during the deposition process a special feature of articulation provided within TMG was used. It allows modeling of rigid body motion of selected elements with respect to the rest of the model. The basic control parameters of the time span for the solution and the result output interval were calculated from the process parameters and the time step was optimized based on the deviation of simulation results from the experimental results to minimize the numerical error. Figure 12 provides the diagrammatic representation of the adopted modeling procedure.

Insert figure 12

5. Application of the developed FEM models

Coupled FEM thermal analysis was carried out, to obtain the numerical solution of temperature field. Following parameters were used in the calculation of the temperature fields during the deposition of Stellite 6 on SS316.

Insert Table 2: Machine input parameters for the deposition of Stellite 6 on SS 316

Insert Table 3: Selected values for the parameters quantifying frictional heat.

The adopted methodology is diagrammatically shown below:

Insert figure 13

The frictional heat generated during the dwell phase as calculated from relation 2, was applied as heat load boundary condition to the frontal surface of mechtrode along with the initial

conditions to the FEM model for the calculated duration. The generated temperature field during the dwell phase was then applied as initial condition to the FEM model along with the heat load calculated from relation 4 for the duration of the deposition phase.

5.1 Comparison between simulation and experimental results

The plots indicate the simulation and experimental temperature response at each of the four locations on substrate.

Insert figure14

Insert figure 15

The maximum temperature values obtained at thermocouples during experimentation were plotted against the results from simulation to ascertain the deviation. The comparison of absolute maximums showed a max error of 18% at location three (figure 15), which is within the acceptable limits.

6. Conclusions

1. The approach of coupled transient thermal analysis to account for the temperature fields generated during the dwell and deposition phases of the process resulted in reasonably accurate results, with an error of 18% between absolute maximums.
2. The major discrepancy between the experimental and simulated results occurred at locations with a change in substrate geometry. This indicates that more accurate representation of the process is required. The heat distribution profile at the frictional interface and variation in material properties with temperature could have significant effects on the thermal response.
3. The validated numerical model could be used to predict bond interface temperature and relations between the machine input parameters, the bond interface temperature and the process response (coating thickness, width and strength) could be established. This would allow for accurate selection of machining parameters for optimum process response.

Acknowledgements

The authors would like to acknowledge the support of EU grant CRAFT – 1999 -70658 "Friction surfacing for multisectorial applications" and the participating companies including Frictec Ltd., Circle Technical Services Ltd, Nordseetaucher GmbH and Neos Robotics.

References

[1] Bedford, G. M. Friction surfacing for wears applications, Metals and Materials, 6(11) (1990), 702-705.

[2] Bedford, G. M., Vitanov, V. I. and Voutchkov, I. I. On the thermo-mechanical events during friction surfacing of high speed steels, Surface and Coating Technology, 141(2001), 34-39.

[3] Cline, H. E. and Anthony, T.R. Heat treating and melting material with a scanning laser or electron beam, Journal of Applied Physics, Vol 48, No. 9, (1977), 3895-3900.

[4] Gratzke, U., Kapadia, P.D. and Dowden, J., Heat Conduction in high-speed laser welding. Journal of Physics and Applied Physics, Vol. 24, No.12, (1991), 21252134.

[5] Komanduri, R., and Hou, Z.B., Thermal analysis of the arc welding process. In Metallurgical and Materials Transactions B (part 1), Vol. 31B, (2000), 13531370.

[6] Kou, S. Welding, glazing and heat treating-a dimensional analysis of heat flow, AMS, Metallurgical Transactions, Vol. 13a, (1982), 363-369.

[7] Kragelsky, V. I., Dobychin, M. and Kombalov, V., Friction and Wear Calculation Methods, Pergamon Press Ltd., England, 1982.

[8] Nguyen, N. T., Analytical solutions for transient temperature of semi-infinite body subjected to 3-d moving heat source, Welding Journal, (1999), 265-274.

[9] Pavelic, V., Tanbakuch, O.A., Ujehara, O.A. and Myers, P.S., Experimental and computed histories in Gas tungsten arc welding thin plates, Welding Journal, Vol. 48, No. 7 (1969), 295-305.

[10] Rabinowicz, Ernest Friction and Wear of Materials, Second Edition, John Wiley and Sons, Inc., 1995.

[11] Shinoda, T., Takemoto, S., Kato, Y., Shimuzu, T., and Yashiro, T., Surface Modification by Friction Surfacing. In*:* Proceedings of the International Thermal Spray Conference'95, Kobe, Japan, May, 1995

[12] Shinoda, T. Deposition of Non-dilution Hard Coating Layer by Friction Surfacing. Denki Seiko (electric furnace steel, Japan), 67(3), 1996, 171-177.

[13] Shinoda, T. et al. Effect of process parameters during friction coating on properties of non-dilution coating layers. Surface Engineering, 14 (3), (1998), 211-216.

[14] Vishnu, P. R. et al., Heat flow for pulsed welding, The Institute of Metals, Materials Science and Technology, Vol. 7, (1991), 649-659.

Nomenclature

V_x	Substrate traverse speed	M_{dwell}	Total frictional moment about the axis of rotation during the dwell phase
V_z	Mechtrode vertical speed	P_{dwell}	Total power expended during the dwell phase
N	Mechtrode rotational speed	M_{depo}	Total frictional moment about the axis of rotation during the dwell phase
V_{zo}	Mechtrode touch down vertical speed	P_{depo}	Total power expended during the deposition phase
N_o	Mechtrode touch down rotational speed	S	Bond Strength
Z_o	Mechtrode touch down depth	T	Coating thickness
X	Length of the run (centre to centre distance)	W	Coating Width
K_{sub}	Thermal Conductivity	μ_o	Coefficient of static friction
ρ_{sub}	Mass Density	p	Frictional pressure
Cp_{sub}	Specific Heat	ω	Angular velocity
K_{coat}	Thermal Conductivity	r	Instantaneous moment arm
ρ_{coat}	Mass Density	c	Empirical coefficient related to the materials involved in interaction
Cp_{coat}	Specific Heat	χ	Coefficient defining the relative magnitude of the instantaneous frictional components
F_n	Normal force	η	Variable dependent on R, c, and ω
R_{eff}	Effective frictional radius	Δz	Mechtrode step change
Q_{dwell}	Fictional heat load during dwell phase	Δx	Deposit step change/
Q_{depo}	Fictional heat load during deposition phase	Δt	Calculation Interval

Table 1

Material	Symbol	Value	Units
Substrate	K_{sub}	16.260	W/m °C
	ρ_{sub}	8.0272E03	Kg/m3
	Cp_{sub}	502.10	J/Kg °C
Coating	K_{coat}	14.644	W/m °C
	ρ_{coat}	8.260E03	Kg/m3
	Cp_{coat}	418.40	J/Kg °C

Table 2

Symbol	Value	Units
V_x	70 (1.1667)	mm/min (mm/sec)
V_z	25 (0.4167)	mm/min (mm/sec)
N	1000 (104.72)	rpm (rad/sec)
V_{zo}	15 (0.25)	mm/min (mm/sec)
N_o	1000 (104.72)	rpm (rad/sec)
Z_o	1.5	mm
X	30	mm

Table 3

Symbol	Range	Sel. Value	Units
Fn	2706.6 ~2813.8	2760.2	N
R_{eff}		3.017	mm
Q_{dwell}	171.0 ~ 177.8	174.4	W
Q_{depo}	153.0 ~ 160.8	156.9	W

List of figures

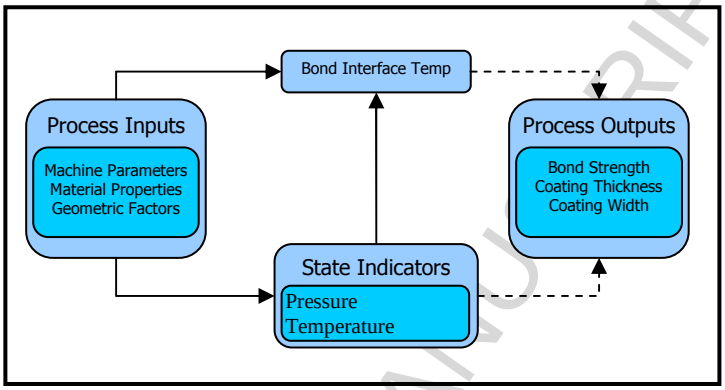

Fig.1. Diagrammatic representation of process parameters

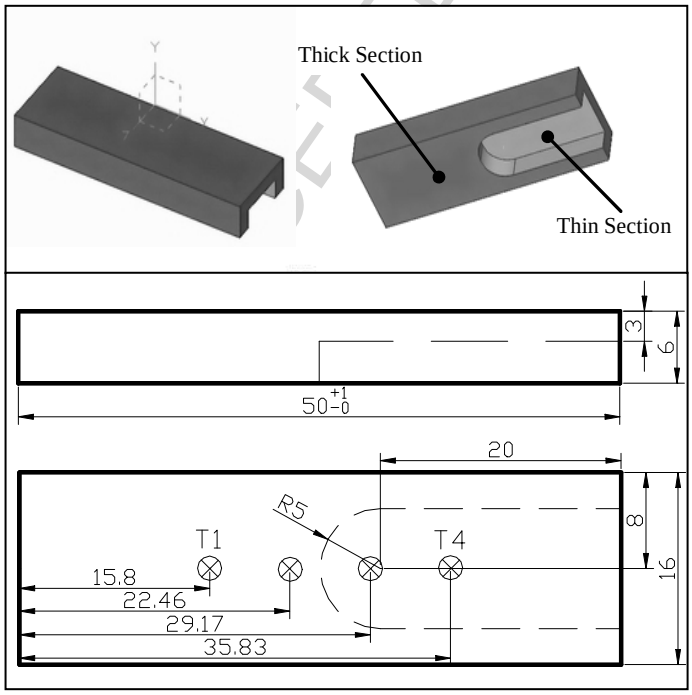

Fig.2. Substrate shape prepared for experimentation and subsequent thermal analysis, and the location of thermocouples.

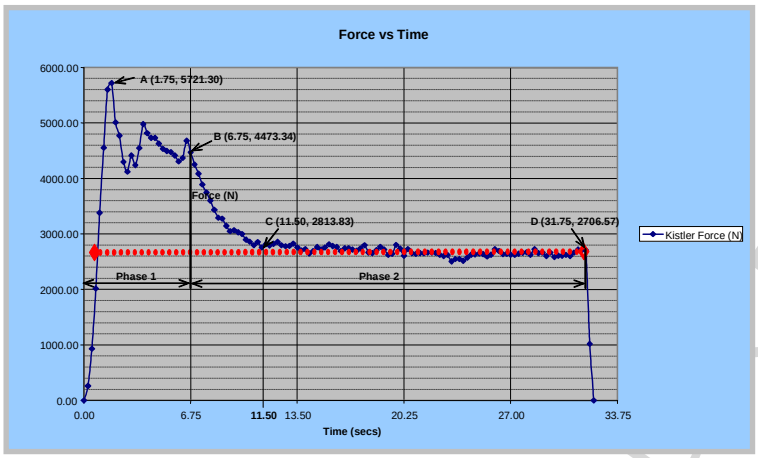

Fig. 3. Force- time plot for the deposition of Stelite 6 on Stainless Steel 316.

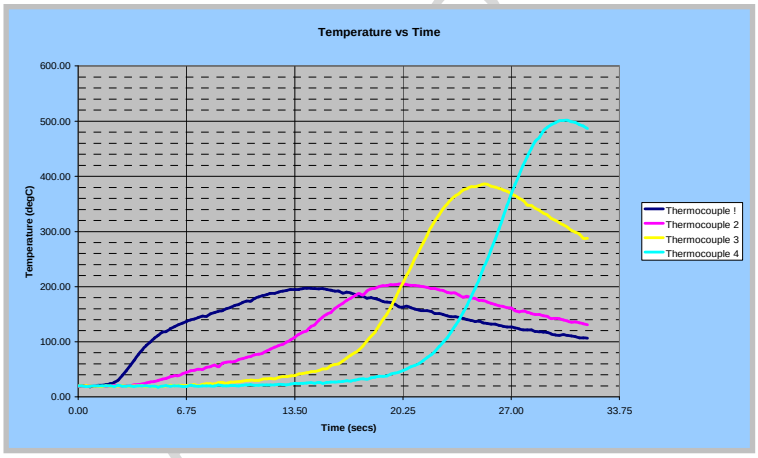

Fig. 4. Experimental temperature response of the system plotted against process time

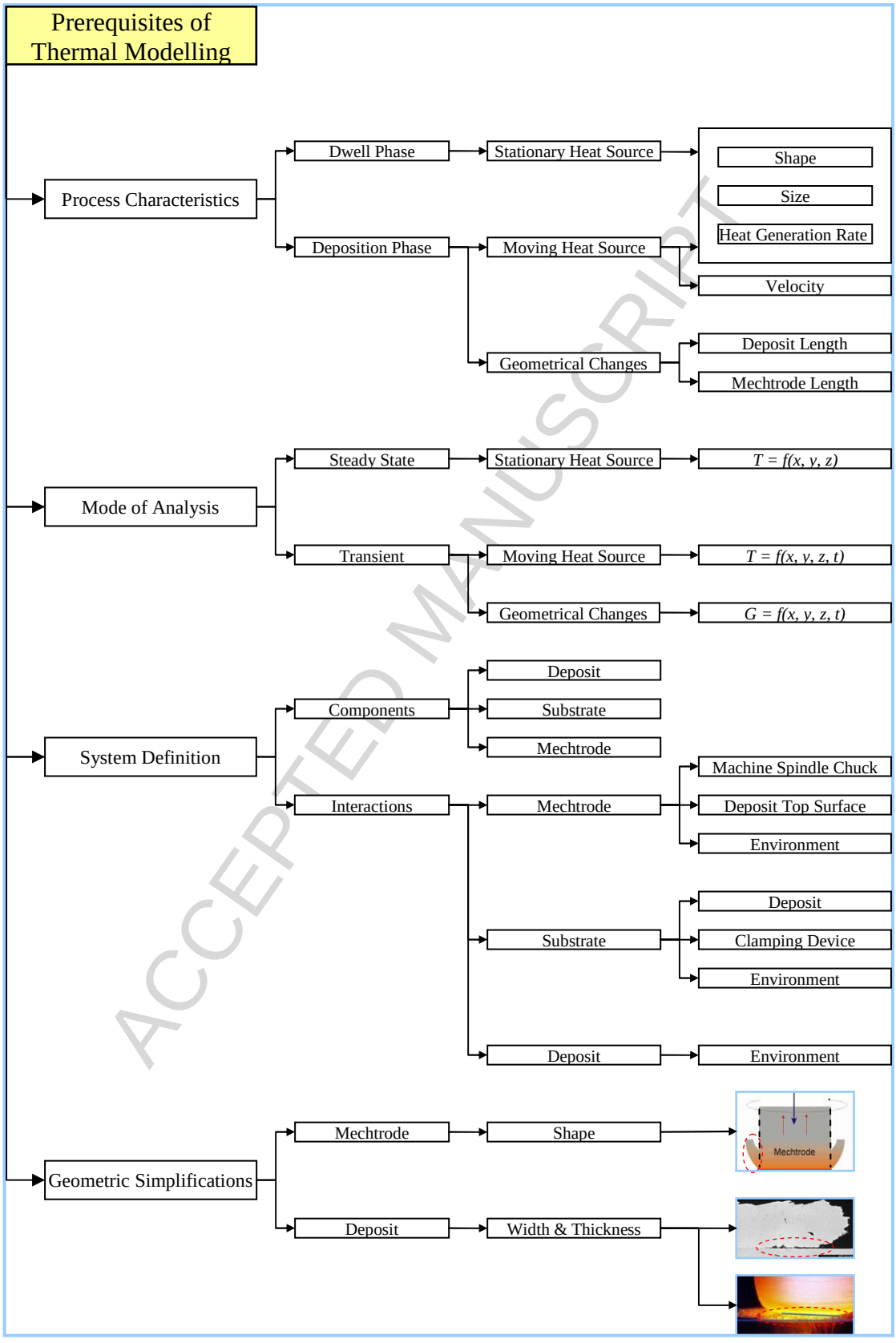

Fig.5 Representation of the factors that were considered before modelling the process

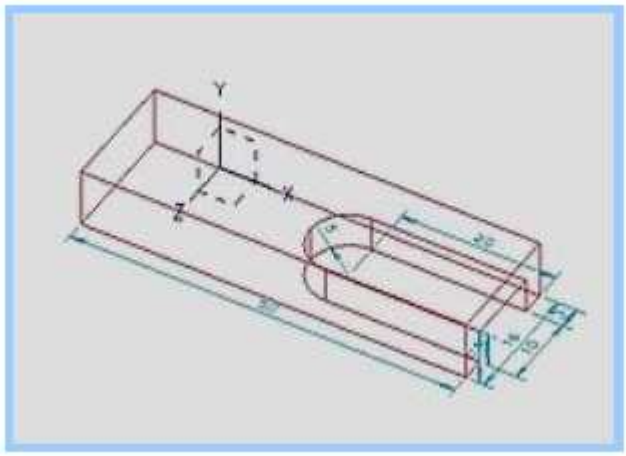

Fig. 6 Shapes and dimension of substrate.

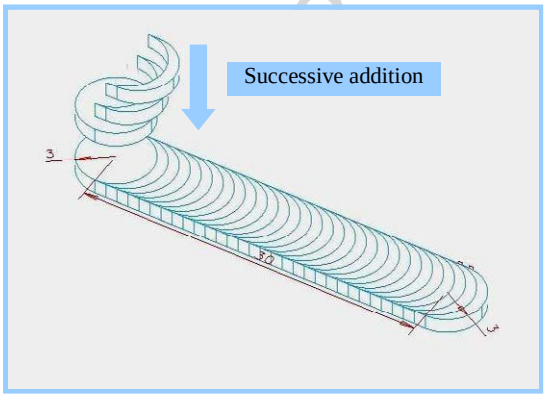

Fig.7. Composite geometric model of deposit layer and substrate

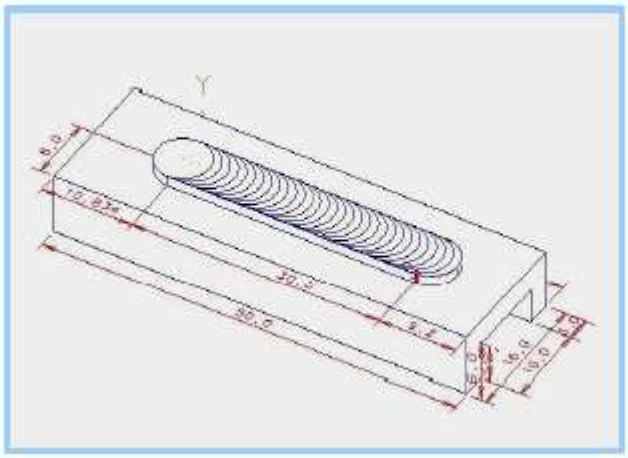

Fig.8. Dimensions of deposit layer.

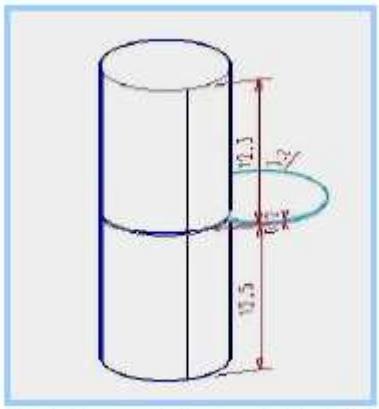

Fig.9. Geometric model of the mechtrode.

Fig.9. Geometric model of the mechtrode.

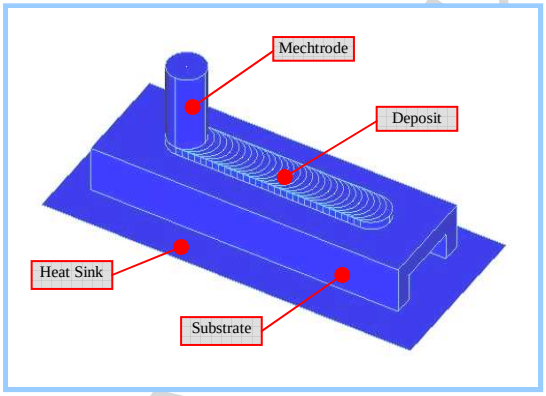

Fig.10. Geometric model of the friction surfacing system.

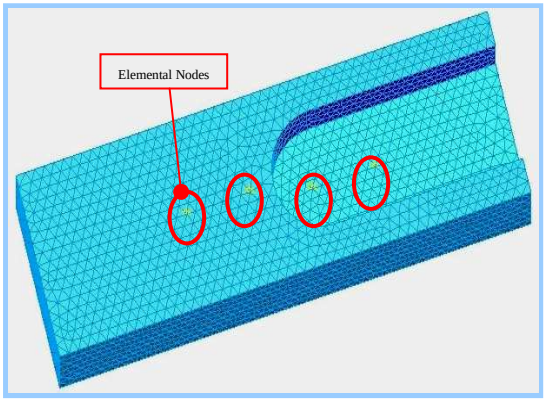

Fig.11. Finite element model of the substrate, showing the placement of element nodes on the pre-positioned anchor nodes.

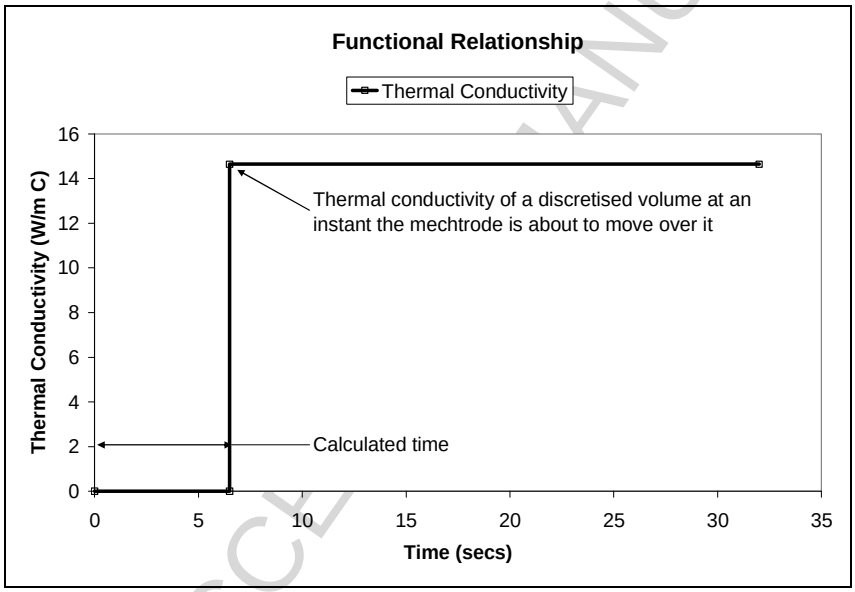

Fig.12. Functional relationship between the thermal conductivity of the deposit and time step.

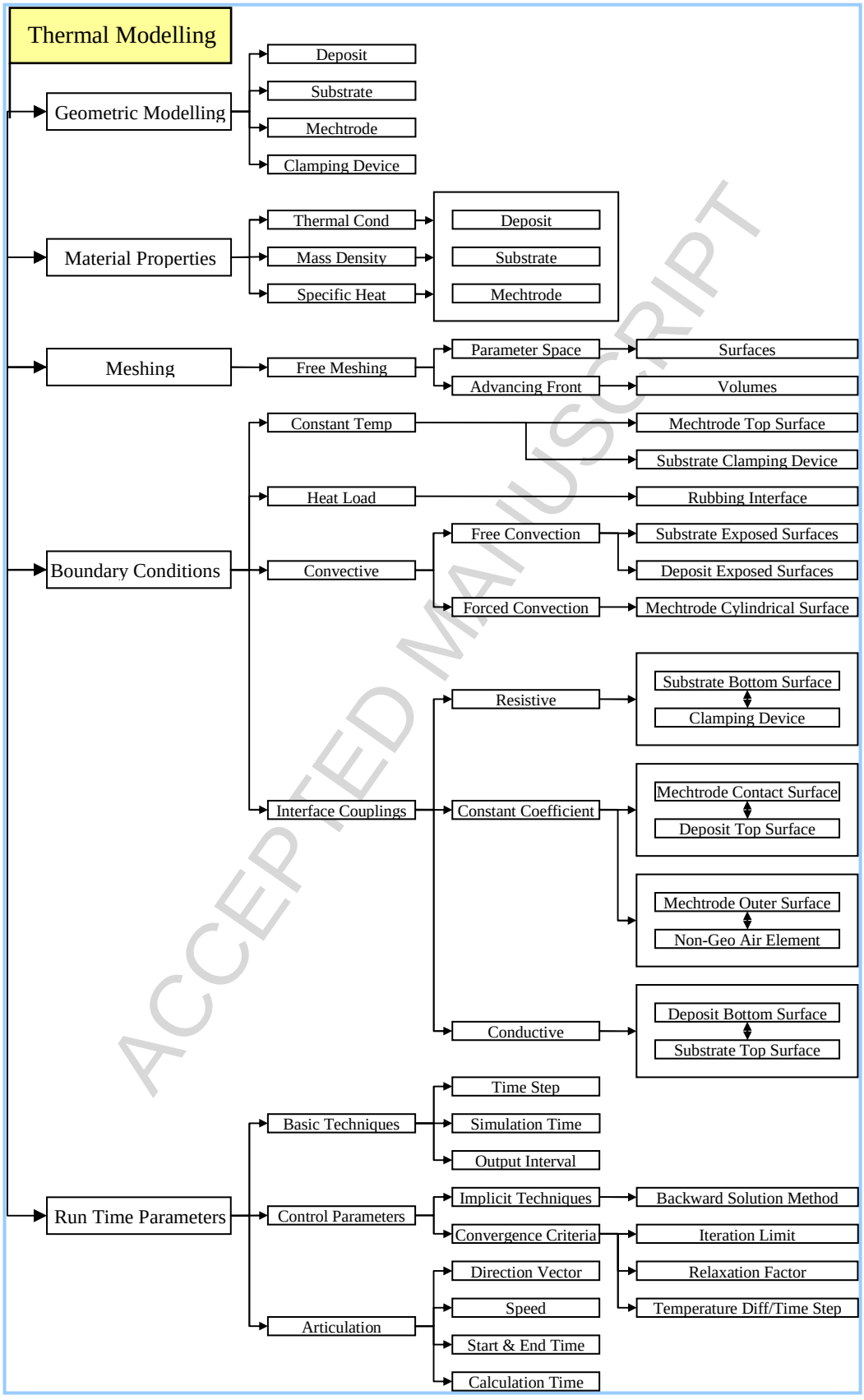

Fig. 13 Thermal modelling procedure

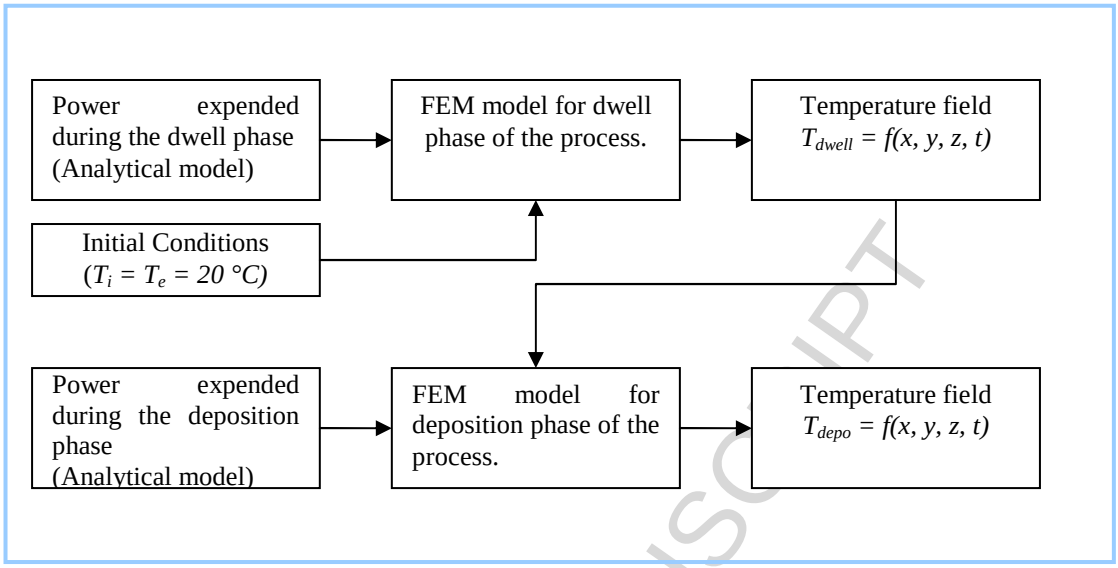

Fig.14. Adapted procedure for evaluating temperature response of the system.

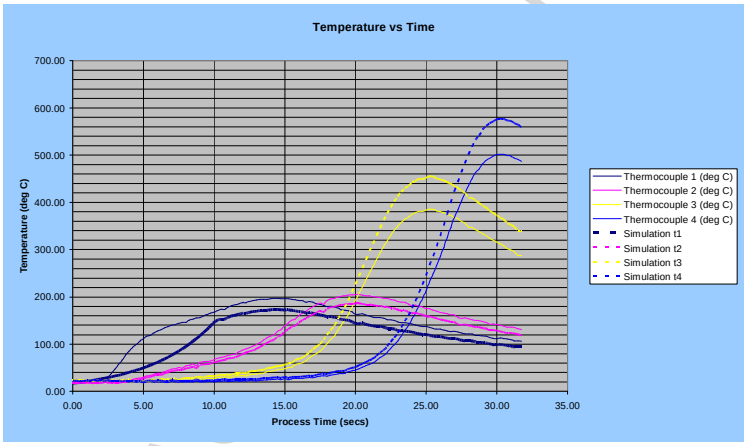

Fig.15. Experimental and simulation temperature response of the system plotted against process time.